Flexibility of $CuCl_4$-tetrahedra in Bis[Cinchoninium Tetrachlorocuprate(II)]trihydrate Single Crystals. X-ray Diffraction and EPR Studies

A. Wesełucha-Birczyńska,*[,1a] B. J. Oleksyn,[1b] S. K. Hoffmann,*[,1c] J. Śliwiński,[1b] B. Borzęcka-Prokop,[1b] J. Goslar,[1c] and W. Hilczer[1c]

Regional Laboratory of Physicochemical Analyses and Structural Research and Faculty of Chemistry, Jagiellonian University, Ingardena 3, 30−060 Kraków, Poland, and Institute of Molecular Physics, Polish Academy of Sciences, Smoluchowskiego 17, 60−179 Poznań, Poland

Received December 12, 2000

Crystal structure of bis[cinchoninium tetrachlorocuprate(II)] trihydrate, $[(C_{19}H_{24}N_2O)CuCl_4]_2 \cdot 3H_2O$, has been determined by X-ray diffraction at 100 K and reexamined at 293 K. The compound crystallizes in orthorhombic system with a $P2_12_12_1$ space group and unit cell parameters $a = 15.3031(14)$, $b = 36.415(3)$, and $c = 7.8341(5)$ Å at 100 K, and $Z = 4$. The asymmetric unit consists of two $(CuCl_4)^{2-}$ tetrahedral anions linked by hydrogen bonds to two doubly protonated cinchonine molecules and three water molecules. The tetrahedra are strongly flattened, to approximately D_{2d} symmetry, with different deformation for two inequivalent $(CuCl_4)^{2-}$ -ions in the asymmetric unit. The deformation of $(CuCl_4)^{2-}$ and cinchoninium cations varies with temperature due to a rearrangement of the bifurcated hydrogen bond network. This is a continuous process observed as a monotonic variation of the EPR spectral parameters and the unit cell dimensions. EPR spectra show that very weak exchange coupling $J_{12} = 0.0030$ cm^{-1} operates between Cu^{2+} ions within asymmetric units, corresponding to the general formula of the compound, as well as between equivalent Cu^{2+} sites of different molecules, whereas the coupling is negligible between inequivalent sites. The intermolecular J_{12} coupling is temperature-independent indicating that the whole asymmetric unit behaves as a magnetic unit (pseudodimer) in the whole temperature range.

Introduction

Cinchonine (cin = $C_{19}H_{22}N_2O$, Scheme 1) is one of the alkaloids of the *Cinchona* tree bark with well recognized antimalarial activity.[2] Double protonation of cin gives the cinchoninium cation, $(cinH_2)^{2+}$, which easily forms hydrated crystalline salts with anions $(MCl_4)^{2-}$ (M = Cd, Co, Zn, Cu, Hg). These moieties are interconnected by hydrogen bond systems in which protons are delivered by −N−H and −O−H groups of cinchoninium cation and water molecules.[3−5] Paramagnetic compounds of $(cinH_2)^{2+}(MCl_4)^{2-} \cdot nH_2O$ are the Curie-paramagnets since, due to a good separation of the $(MCl_4)^{2-}$-complexes by large cinchoninium cations, the superexchange coupling between paramagnetic ions is negligible or very small both in $(cinH_2)^{2+}(CoCl_4)^{2-} \cdot 2H_2O$ [6] and in $[(cinH_2)^{2+}(CuCl_4)^{2-}]_2 \cdot 3H_2O$.[7] This enables us to apply EPR to study electronic and geometrical structures of individual $(MCl_4)^{2-}$ tetrahedra and to get information supplementary to the X-ray diffraction data. The anion structure, especially for tetrachlorocuprates(II), displays a geometry varying between tetrahedral and square planar limits mostly with compressed (flattened) tetragonal D_{2d} symmetry.[8] The degree of deformation can be described by a flattening angle β between the deformation axis and Cu−Cl bond. In T_d symmetry $\beta = 54.74°$ and in planar geometry D_{4h} $\beta = 90°$. Another deformation parameter usefull for very irregular tetrahedra is $D = (L_3 - L_1)/(L_1 + L_2 + L_3)^{1/3}$ where L_i are distances between the centers of opposite tetrahedron edges and $L_1 < L_2 < L_3$.[9] For T_d symmetry $D = 0$.

Scheme 1

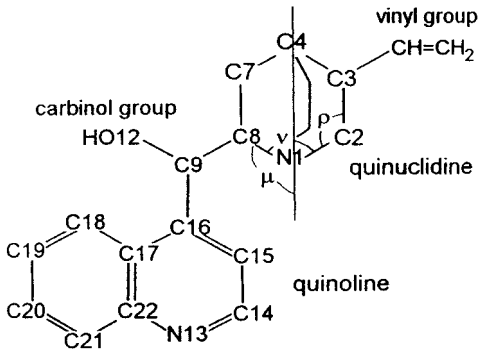

The flattening of a free $(CuCl_4)^{2-}$-tetrahedron is its internal property, and the equilibrium geometry appears at $\beta = 60°$ as

* To whom correspondence should be addressed. Fax (+48)-12-6343859. E-mail: birczyns@chemia.uj.edu.pl.

(1) (a) Regional Laboratory, Jagiellonian University. (b) Faculty of Chemistry, Jagiellonian University. (c) Institute of Molecular Physics, Polish Academy of Sciences.
(2) Hofheinz, W.; Merkli, B. Quinine and Quinine Analogues. In *Handbook of Experimental Pharmacology*; Peters, W., Richards, W. H. G., Eds.; Springer-Verlag: Berlin, 1984; Vol. 68/II.
(3) Oleksyn, B. J.; Stadnicka, K. M.; Hodorowicz, S. *Acta Crystallogr.* **1978**, *B34*, 811.
(4) Chojnacki, J.; Oleksyn, B. J.; Hodorowicz, S. *Rocz. Chem.* **1975**, *49*, 429.
(5) Oleksyn, B. J.; Stadnicka, K. M.; Hodorowicz, S. *Rocz. Chem.* **1976**, *50*, 1645.
(6) Drulis, H.; Dyrek, K.; Hoffmann, K. P.; Hoffmann, S. K.; Wesełucha-Birczyńska, A. *Inorg. Chem.* **1985**, 24, 4009.
(7) Dyrek, K.; Goslar, J.; Hodorowicz, S. A.; Hoffmann, S. K.; Oleksyn, B. J.; Wesełucha-Birczyńska, A. *Inorg. Chem.* **1987**, *26*, 1481.
(8) Halvorson, K. E.; Patterson, C.; Willett, R. D. *Acta Crystallogr.* **1990**, *B46*, 508.
(9) Lamotte-Brasseur, J.; Van den Bossche, G. *Acta Crystallogr.* **1974**, *A30*, 484.

10.1021/ic001402a CCC: $20.00
Published on Web 07/28/2001

a result of a balance between crystal field stabilization favoring D_{4h} geometry and electrostatic repulsion between chlorine atoms favoring D_{2d} geometry.[10] The $(CuCl_4)^{2-}$ anion is precluded also from adopting a regular tetrahedral T_d geometry by the Jahn−Teller effect. Planar $(CuCl_4)^{2-}$ geometry is forced in crystals with strong hydrogen bonding between large organic molecules and chlorine atoms.

The various degree of pseodotetrahedral deformation have been attributed to the nature of the counterions and the strength of the hydrogen bonding. Also the dynamics of the tetrahedra, their excitations to higher vibrational levels, and lattice dynamics can influence the $(CuCl_4)^{2-}$geometry. $(CuCl_4)^{2-}$ has a very shallow minimum of the potential surface and thus the position of the minimum is very sensitive to even small changes in the intermolecular interactions and dynamics as evidenced by the abnormally large red shift of the d−d absorption bands on warming.[11] This can lead to a static or dynamic disorder influencing apparent $(CuCl_4)^{2-}$ geometry. A flexibility of pseudotetrahedral $(CuCl_4)^{2-}$ geometry leads to the thermochromic properties. Thermochromic transmission can be continuous or discontinuous, reversible or irreversible and occurs, as a rule, above ambient temperature.[12] Thermally activated changes of the pseudotetrahedral deformation can also appear over large range of temperatures without remarkable changes in the color of a compound, but it is observed as continuous temperature variations of EPR *g*-factors as found in tetrachlorocuprate(II) salts of aminopyridinium.[13] Such a situation seems to exist in $[(cinH_2)^{2+}(CuCl_4)^{2-}]_2{\cdot}3H_2O$ crystals which change continuously the color from yellow-green at room temperature to green at liquid nitrogen temperature (77 K). Temperature-induced changes were also observed in the far FT-IR spectra measured in temperature range 10−295 K and were explained as due to a deformation of the $(CuCl_4)^{2-}$ anion as well as changes in the hydrogen bond network.[14]

In the previous paper[7] we reported the single crystal structure of this compound determined at room temperature using X-ray diffraction. Only 38 hydrogen atoms from the total number of 58 were found and their positions were not refined because of computer memory limitations. The EPR data, contained in the same paper, indicated a very weak exchange coupling between Cu^{2+} ions and the powder EPR spectra behavior suggested that the coupling is temperature dependent.

In this paper we present the crystal structure of $[(cinH_2)^{2+}(CuCl_4)^{2-}]_2{\cdot}3H_2O$ at low temperature (100 K) and redetermined at room temperature (293 K) in order to follow the temperature influence on the hydrogen bonding and the shape of $(CuCl_4)^{2-}$ tetrahedra. The hydrogen bond network seems to be remarkably dense near $(CuCl_4)^{2-}$ tetrahedra in this crystal and changes at low temperature. To look closely on temperature effects in the electronic structure of $(CuCl_4)^{2-}$-tetrahedra, their relation to the structural data, and superexchange between Cu^{2+}-ions we have performed detailed temperature studies of single-crystal EPR spectra at various crystal orientations.

Experimental Section

Synthesis of the compound (Cu−cin) was described previously.[15]

EPR Measurements. Single-crystal EPR measurements were performed on a BRUKER ESP 380E FT/CW spectrometer operating at X-band in CW-mode with corrundum TE_{011} resonator and equipped with an OXFORD CF 935 flow helium cryostat.

Table 1. Crystal Data and Structure Refinement for Bis[cinchoninium tetrachlorocuprate(II)] Trihydrate at Low and Room Temperatures

empirical formula	$C_{38}H_{54}Cl_8Cu_2N_4O_5$	
formula weight	1057.53	
temperature	100.0(2) K	293(2) K
wavelength	1.54180 Å	
crystal system, space group	orthorhombic, $P2_12_12_1$ (No. 19)	
unit cell dimensions		
a (Å)	15.3011(14)	15.3948(16)
b (Å)	36.415(3)	36.695(7)
c (Å)	7.8341(5)	7.9806(7)
α (deg)	90	90
β(deg)	90	90
γ (deg)	90	90
volume (Å^3)	4365.0(6)	4508.4(10)
Z	4	4
calculated density, D_{calcd} (gcm^{-3})	1.609	1.558
absorption coefficient, μ (mm^{-1})	6.096	5.902
$R(F_o)$, all data[a]	0.0482	0.0713
$R_w(F_o^2)$, all data[a]	0.1237	0.1918
absolute structure parameter	0.053(12)	0.04(2)

[a] Discrepancy factors are defined as $R = \sum||F_o| - |F_c||/\sum|F_o|$. $R_w = \{\sum[w(F_o^2 - F_c^2)^2]/\sum[w(F_o^2)^2]\}^{1/2}$.

Single-Crystal X-ray Structure Analysis. Crystal data and details of the X-ray structure analysis are given in Table 1. Intensity data collection was performed on a four-circle automated KM-4 diffractometer (KUMA Diffraction, Wrocław, Poland) equipped with the cooling device, Cryostream Cooler (Oxford). The graphite-monochromated copper radiation and $\omega/2\Theta$ scan mode was used during the measurements performed at 100 K (LT) and 293 K (RT). For each temperature the intensities of three standard reflections were monitored after every 50 measurements. They remained constant to within 3.5% for LT and 5.7% for RT. The data were corrected for Lorentz and polarization effects but not for absorption. The phase problem was solved with direct methods using SHELXS (part of SHELX97 system[16]) program on F^2 values. The difference Fourier map calculated subsequently revealed all non-hydrogen atoms and the absolute configuration of cinchonine molecule, C3−R, C4−S, C8−R, C9−S, was that corresponding to the natural compound. All hydrogen atoms were found on difference Fourier maps after subsequent anisotropic refinement of all heavier atoms and refined isotropically using riding model. The refinement was carried out using SHELXL97 program[16] and was based on F^2 values. The final difference Fourier map had no peak higher than 1.14 e/Å^3 (in vicinity of Cu1). The refined parameters of the LT structure were then used as an introductory model for the RT structure refinement. In the case of RT structure the positions of some hydrogen atoms were found in the difference Fourier maps and some of them were calculated and refined with riding model. The highest peak is 1.05 e/Å (in vicinity of Cu1).

Temperature Powder X-ray Diffraction (PXRD) Studies. X-ray powder diffraction pattern of Cu−cin was recorded in the range of 295−143 K (cooling) with a Philips PW1710 diffractometer using Ni filtered Cu Kα (40 kV/30 mA) radiation (λ = 1.54178 Å), with a step scan mode: step size = 0.02° [2θ], time per step = 2 [s]. A positional calibration of the goniometer was checked before the experiment with a hexagonal α-quartz standard (a_h = 4.9132(2) Å, c_h = 5.4058(3) Å). The corrections for systematic $\Delta 2\Theta$ were applied. Indexing of the patterns was performed by the POWDER[17] program, and lattice parameters were refined with LSQ procedure described by Appleman et al.[18]

(10) Elian, M.; Hoffmann, R. *Inorg. Chem.* **1975**, *14*, 1058.
(11) McDonald, R. C.; Hitchman, M. A. *Inorg. Chem.* **1986**, *25*, 3273.
(12) Bloomquist, D. R.; Willett, R. D. *Coord. Chem. Rev.* **1982**, *47*, 125.
(13) Gaura, R. M.; Stein, P.; Willett, R. D.; West, D. X. *Inorg. Chim. Acta* **1982**, *60*, 213.
(14) Wesełucha-Birczyńska, A.; Oleksyn, B.; Paluszkiewicz, C.; Śliwiński, J. *J. Mol. Struct.* **1999**, 511−512, 301.
(15) Dyrek, M. *Rocz. Chem.* **1976**, *50*, 2027.
(16) Sheldrick, G. M. *SHELX97, Program for the Refinement of Crystal Structures*; University of Göttingen: Germany, 1997.
(17) Taupin, D. G. *J. Appl. Crystallogr.* **1969**, 179.
(18) Appleman, D. W.; Handwerber, D. S.; Evans, H. T. *Program X-ray, Geological Survey*; US Department of the Interior: Washington, DC, 1966.

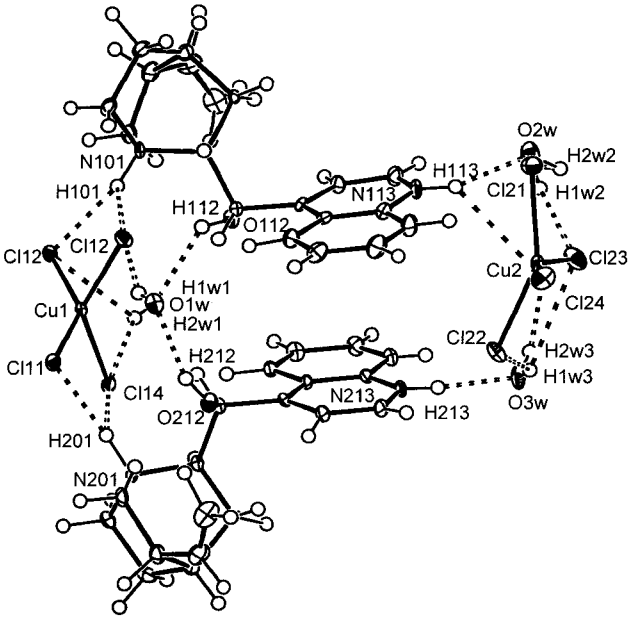

Figure 1. Projection of the asymmetric unit of $[(cinH_2)^{2+}(CuCl_4)^{2-}]_2 \cdot 3H_2O$ along *the c*-axis at 100 K. Atom numbers in cin1 and cin2 are preceded by 1 and 2, respectively; for detailed numbering look in Scheme 1. Displacement elipsoids are drawn at the 50% level; hydrogen atoms are represented by spheres of arbitrary size.

Results and Discussion

Description of the Structure. The projections of the asymmetric unit and of the unit cell of the title compound (Cu−cin) along *c*-axis at 100 K are shown in Figure 1 and Figure 2, respectively. The asymmetric unit was chosen in a way different from that in the previous paper.[7] The new choice turned out to be adequate to the chemical character of the substance, since it shows two cinchoninium cations of $(cinH_2)^{2+}$ linked to two tetrachlorocuprate anions, $(Cu1Cl_4)^{2-}$, $(Cu2Cl_4)^{2-}$, and to three water molecules via intermolecular hydrogen bonds.

Tetrachlorocuprate anions $(CuCl_4)^{2-}$. The geometry of $(CuCl_4)^{2-}$ anions at 100 K is shown in Figure 3. The coordination polyhedra of Cu atoms may be described as distorted tetrahedra. The parameters characterizing the shape of $CuCl_4$ tetrahedra are listed in Table 2. At low temperature the Cu−Cl bond lengths for Cu1 and Cu2 are comparable to within 0.01 and 0.04 Å, respectively, but the range of their differences is much higher than estimated 3σ. The bond angles 2β, Cl−Cu1−Cl, differ significantly from tetrahedral angle ($2\beta_T = 109.48°$) and vary from 95.29(4)° to 144.07(4)°. The flattening is even stronger in $(Cu2Cl_4)^{2-}$, where the range of the bond angles is from 92.24(4)° to 153.74(4)°. At room temperature the Cu−Cl bond lengths in both tetrahedra do not change significantly, while Cl−Cu2−Cl bond angles become more similar to those of Cl−Cu1−Cl, their ranges being 93.48(9)°−148.04(10)° and 95.19(6)°−144.95(7)°, respectively.

The values of distances L_i between the centers of the opposite tetrahedral edges, being a measure of the tetrahedra flattening, confirm the much stronger distortion of $(Cu2Cl_4)^{2-}$. Also the effective deformation parameters *D* of $(Cu2Cl_4)^{2-}$ tetrahedra are greater than those of $(Cu1Cl_4)^{2-}$ at both temperatures. The values of *D* increase when passing from 100 to 293 K, but the tetrahedron $(Cu2Cl_4)^{2-}$ is more sensitive to the change of temperatures than $(Cu1Cl_4)^{2-}$. The deformation parameter *D* is large compared to other Cu(II) compounds [8] showing remarkable compression of the $(CuCl_4)^{2-}$ tetrahedra.

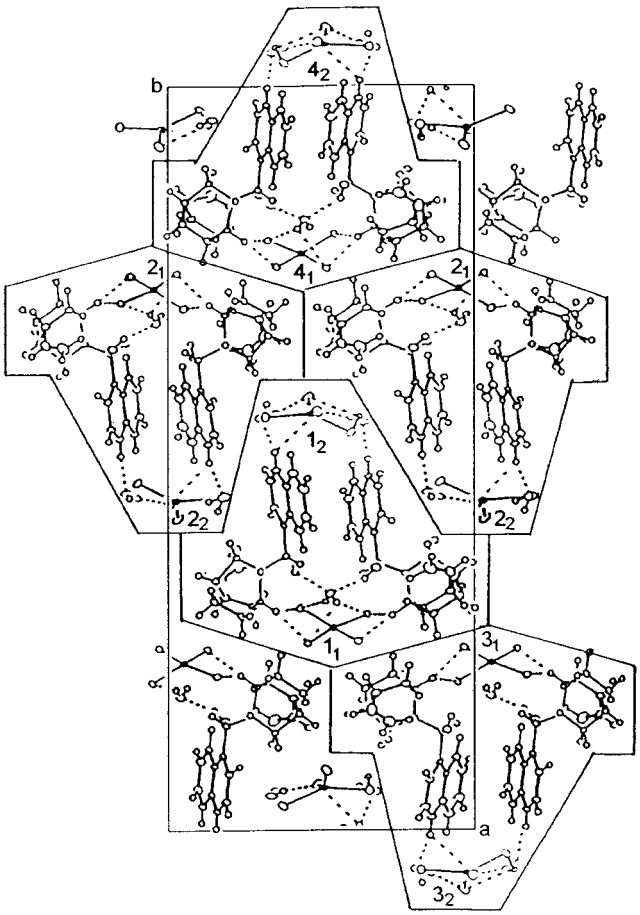

Figure 2. Projection of the unit cell along *c*-axis at 100 K. The cages contain single molecules $[(cinH_2)^{2+}(CuCl_4)^{2-}]_2 \cdot 3H_2O$ marked as 1−4 with two geometrically inequivalent $(CuCl_4)^{2-}$ anions marked by subscripts 1 and 2. The cages 1−2 and 3−4 form two-dimensional planes parallel to the *ac*-plane coupled by dispersive forces only.

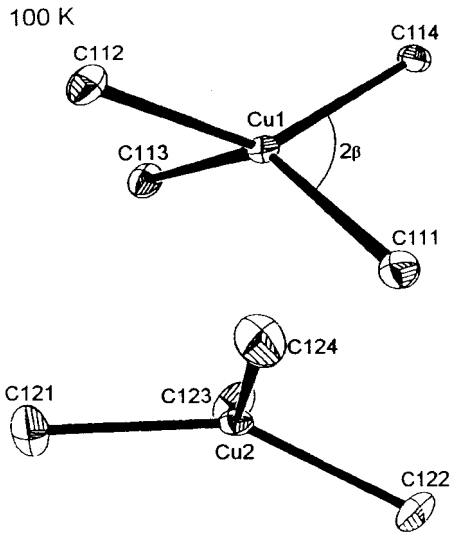

Figure 3. Geometry of $(CuCl_4)^{2-}$ at 100 K in projection on (001) plane.

Cinchoninium Cations $(cinH_2)^{2+}$. The corresponding bond lengths and bond angles in both cations, cin1 and cin2, at both temperatures are comparable to within 3σ values.

Influence of Protonation on the Molecular Geometry of Cinchonine. It is interesting to compare the bond lengths and angles in the protonated quinuclidine moiety with those in the

Table 2. Deformation Parameters of $(CuCl_4)^{2-}$-Tetrahedra at 100 and 293 K

		Deformation angle		Deformation parameters			
anion	temperature	β (deg)[a]		L_1[b]	L_2	L_3	D[c]
$(Cu1Cl_4)^{2-}$	100 K	72.04	69.36	1.490	2.982	3.029	0.786
	293 K	72.48	69.82	1.455	2.995	3.031	0.806
$(Cu2Cl_4)^{2-}$	100 K	76.79	76.40	1.047	3.098	3.113	0.848
	293 K	74.02	73.99	1.238	3.075	3.087	0.949

[a] $\beta = {}^1/_2$(Cl−Cu−Cl), where Cl−Cu−Cl > 109.54°. In T_d symmetry of $(CuCl_4)^{-2}$ $\beta = 54.74°$and $D = 0$. [b] L_i are distances between centers of opposite tetrahedron edges in Å. [c] $D = (L_3 - L_1)/(L_1 + L_2 + L_3)^{1/3}$, when $L_1 < L_2 < L_3$.

free base molecule of cinchonine.[19] The N1−C bonds are lengthened on protonation so that the average differences between bonds in the cations and neutral quinuclidine are 0.033(5)−0.025(5) Å. Protonation of the lone electron pair on N1 in the quinuclidine fragment influences the C−N−C (ν) and C−C−N (ρ) angles (Scheme 1): they widened and sharpened, respectively, in comparison to those in the neutral molecule. The changes in the angles μ between the N1···C4 line and N−C bonds on protonation compensate the changes in the angles ν. A similar behavior was noticed earlier for the pairs base/cation for quinine[20] and cinchonine.[21]

The influence of the proton attached to N1 on its direct surrounding can be also estimated by a factor called piramidality:[22]

$$P(\%) = [(360 - \sum \mu_i)/ (360 - 328.40)] \cdot 100\%$$

P(%) is higher when the lone pair resides on N1, as in the case of cinchonine ($P = 110.12\%$). When the lone electron pair is engaged in the bond with proton, the P(%) is lower, its values being comprised in the range of 90.22−93.06%.

The influence of temperature on the geometry of cations on the vicinity of N1 seems to be more visible for cin1 than for cin2.

Protonation of N13 also affects its vicinity as shown by comparison to the geometry of cinchonine base.[19] The bond lengths are not changed significantly but the C14−N13−C22 angle increases by 6°. This is in agreement with the studies of Domenicano and Vaciago [23] concerning the effect of electron withdrawing substituents on the geometry of the aromatic systems. The geometry of the N13 surrounding seems to be temperature independent.

Conformation. The quinoline moieties of cin1 and cin2 are approximately planar to within 0.03 Å at both temperatures. At room temperature the deviation from planarity is slightly weaker. The torsion angles τ_1 = C15−C16−C9−O12, τ_2 = O12−C9−C8−C7, and τ_2' = O12−C9−C8−N1 (Scheme 1, Table 3), which determine the overall shapes of the cinchonine cations, vary between cin1 and cin2 and with temperature. The most significant difference (6−7°) occurs for τ_1, its value being greater in cin1 at both temperatures. This change is probably related to a very noticeable variation (43°) of τ_3 = H12−O12−C9−C8, connected with the different orientations of the H12−O12 bond in cin1 and cin2.

The conformation of the quinuclidine moiety can be characterized by its discrepancy from the ideal D_{3h} geometry. This moiety in the cations cin1 and cin2 at both temperatures has a distorted D_3 symmetry, similar to that in the cin base.[19] The most pronounced twist in the quinuclidine skeleton is observed for the torsion angles involving C8, close to the group −O12−H which is a proton donor in the hydrogen bond system. The torsion angles τ_4 = C4−C3−C10−C11 which represent the behavior of the vinyl substituent are very variable and most probably are determined by packing conditions.

Rigid-Molecule Test of the Cinchonine Cation. The rigid-body motion test was carried out using the PLATON program.[24,25] The results indicate that the molecule can be divided in the two rigid segments, quinuclidine and quinoline. Their most significant mutual motions are those of the C18, C19, and C20 of the quinoline fragment in relation to the whole quinuclidine segment. The vinyl moiety is moving considerably and independently of both rigid moieties. The carbinol group −C9−O12−H, which connects quinuclidine and quinoline, seems to behave as a rigid "joint" between them. The internal molecular motion is similar at low and room temperatures but the atomic displacement parameters have larger amplitudes at higher temperature. There are some differences, however, in the behavior of cin1 and cin2 at room temperature. In cin2 there are more atoms of the quinoline segment engaged in the motions relative to the quinuclidine moiety.

Molecular Packing. The packing of the cations, anions, and water molecules in the structure is dominated by the intermolecular hydrogen bonds. A thorough description of the hydrogen-bond network is difficult because of high experimental errors in the determination of the positions of the hydrogen atoms, especially of those belonging to the water molecules. At room temperature these atoms may suffer a certain degree of disorder. Nevertheless, such description has been undertaken bacause of the very interesting features of the hydrogen bonding, their essential role in the unit cell packing, and their dependence upon temperature. The hydrogen-bond networks at low and room temperature are partially dissimilar as can be seen by comparison of the linkages along the *c*-axis in Figure 4a,b which show the chains of the anions hydrogen bonded to cation fragments and water molecules in the projection on (010). The parameters of the hydrogen bonds and short contacts are specified in Table 4.

Quinuclidine nitrogen atoms N101 and N201 of cin1 and cin2 cations are the proton donors in the bifurcated hydrogen bonds with Cl12, Cl13 and Cl11, Cl14, respectively. In each pair of bonds one is shorter and more linear than the other. Quinoline nitrogen atoms N113 and N213 are proton donors in the hydrogen bonds with water molecules O2W and O3W, respectively. At low temperature the proton H113 of N113 interacts also with Cl24 atom which belongs to the anion $(Cu2Cl_4)^{2-}$ from another asymmetric unit translated by −**c** (Figure 4). The oxygen atoms O112 and O212 form hydrogen bonds with two water molecules O1W and O1W#2, respectively. These water molecules are translated in respect to each other by +**c**. Water molecules OW1 are also engaged in the hydrogen bonds with chlorine atoms. Occurrence of these interactions depends on temperature. At low-temperature, water molecule O1W donates its hydrogen atom H2W1 into bifurcated hydrogen bonds with

(19) Oleksyn, B.; Lebioda, Ł; Ciechanowicz-Rutkowska, M. *Acta Crystallogr.* **1979**, *B35*, 440.
(20) Oleksyn, B. J.; Serda, P. *Acta Crystallogr.* **1993**, *B49*, 530.
(21) Kowalik, J. T.; Lipińska, T.; Oleksyn, B. J.; Śliwiński, J. *Enantiomer* **1999**, *4*, 389.
(22) Häfelinger, G.; Mach, H. G. Enamines: General and Theoretical Aspects. In *The Chemistry of Enamines*; Rappaport, Z., Ed.; John Wiley: New York, 1994; p 13.
(23) Domenicano, A.; Mazzeo, P.; Vaciago, A. *Tetrahedron Lett.* **1976**, 1029. Domenicano, A.; Vaciago, A.; Coulson, C. A. *Acta Crystallogr.* **1975**, *B31*, 221.
(24) Spek, A. L. *Acta Crystallogr.* **1990**, *A46*, C-34.
(25) Rosenfield, R. E., Jr.; Trueblood, K. N.; Dunitz, J. D. *Acta Crystallogr.* **1978**, *A34*, 828.

Table 3. Selected Torsion Angles in Cin1 and Cin2 at Low and Room Temperatures

	cin1		cin2		
	100K	293K	100K	293K	cin (base)
τ_1 = C15−C16−C9−O12	28.5(4)	28.4(7)	22.5(4)	21.1(7)	23.4
τ_2 = O12−C9−C8−C7	−66.1(4)	−65.8(6)	−69.8(4)	−67.0(6)	−50.6
τ_2' = O12−C9−C8−N1	57.4(4)	58.4(6)	54.8(4)	57.2(6)	76.1
τ_3 = H12−O12−C9−C8	−73(5)	−95.9(6)	−116(5)	−90.2(6)	65
τ_4 = C4−C3−C10−C11	108.3(6)	115(11)	126.2(5)	124(1)	−117.1(4)

Cl13 and Cl14, while its another hydrogen atom H1W1 is connected with Cl12#1, translated by −**c**. The water molecule O2W forms a "bridge" between Cl23 and Cl21#1 of different anions (related by **c** translation) with the use of its hydrogen atoms H1W2 and H2W2, respectively. The water molecule O3W joins two chlorine atoms, Cl22 and Cl23 of the same anion, so that they share the same hydrogen atom H1W3. The other hydrogen, H2W3, is accepted by the chlorine atom Cl24#1, of another anion translated by −**c**. Certain function in the molecular packing is also played by interactions between quinoline moieties of the cations within the asymmetric unit. The quinoline rings of cin1 and cin2 are antiparallel to each other so that nitrogen atom N113 is located over C218 and N213 is located over C118 (Figure 1). The distance between the centroids of the rings, taken in the center of C17−C22 bonds is 3.833 Å at low temperature and 3.853 Å at room temperature.

Inspection of the involvement of $(CuCl_4)^{2-}$ anions in the hydrogen bond network shows that the chlorine atoms of $(Cu1Cl_4)^{2-}$ take part in seven and six hydrogen bonds at low and room temperature, respectively, while those of $(Cu2Cl_4)^{2-}$

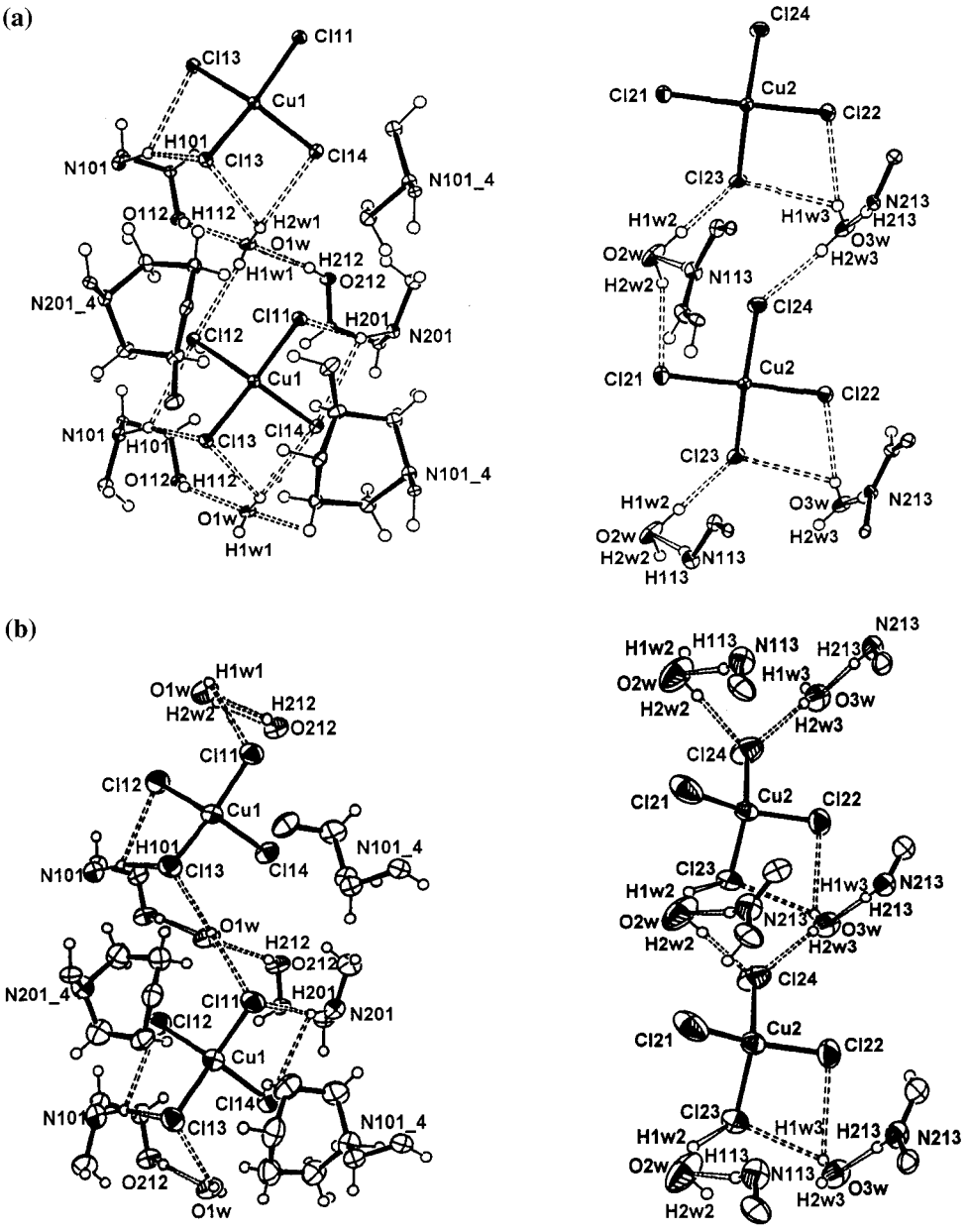

Figure 4. Hydrogen bonding pattern along *c*-axis at (a) 100 K and (b) 293 K. For the sake of clarity, the labels of the equivalent atoms are not given for all positions translated by **c**. _4 designates symmetry transformation: $x + 0.5, -y + 0.5, -z$.

Table 4. Hydrogen Bonds and Short Intermolecular Contacts for Bis[Cinchoniniumtetrachlorocuprate(II)] Trihydrate at Low and at Room Temperatures [Å and deg]

Hydrogen Bonds

	100 K				293 K			
	D−H	H···A	D···A	D−H···A	D−H	H···A	D···A	D−H···A
N101−H101···Cl13	0.99(5)	2.23(5)	3.150(3)	154(4)	1.03(9)	2.21(9)	3.172(5)	153(7)
N101−H101···Cl12	0.99(5)	2.83(5)	3.468(3)	123(4)	1.03(9)	2.88(9)	3.521(6)	121(6)
O112−H112···O1W	0.70(6)	2.18(6)	2.741(4)	138(6)	0.63(10)	2.22(11)	2.770(7)	146(13)
N113−H113···O2W	0.93(6)	1.90(6)	2.792(4)	161(5)	0.74(11)	2.21(11)	2.818(8)	140(11)
N113−H113···Cl24#1	0.93(6)	3.00(6)	3.575(3)	122(4)				
N201−H201···Cl11	1.10(5)	2.15(5)	3.178(3)	154(4)	0.95(9)	2.39(9)	3.192(5)	142(7)
N201−H201···Cl14	1.10(5)	2.81(5)	3.501(3)	121(3)	0.95(9)	2.84(9)	3.509(6)	129(6)
O212−H212···O1W#2	0.82(6)	1.97(6)	2.752(4)	159(5)	0.82	1.99	2.797(7)	168.3
N213−H213···O3W	0.87(5)	1.83(5)	2.695(4)	173(5)	0.60(10)	2.15(10)	2.739(7)	169(13)
O1W−H1W1···Cl12#1	0.71(6)	2.56(6)	3.223(3)	157(6)				
O1W−H1W1···O212#1					0.93	2.10	2.797(7)	131.2
O1W−H2W1···Cl14	0.70(6)	2.66(6)	3.305(3)	154(6)				
O1W−H2W1···Cl13	0.70(6)	2.98(6)	3.403(3)	122(6)	1.05	2.80	3.420(5)	118.0
O1W−H2W1···Cl11#1					1.05	2.96	3.515(5)	113.6
O2W−H1W2···Cl23	1.04(8)	2.40(8)	3.430(4)	172(6)	0.78	2.95	3.472(11)	126.8
O2W−H2W2···Cl21#1	1.01(7)	2.72(7)	3.323(4)	119(5)				
O2W−H2W2···Cl24#1					0.87	2.30	3.082(7)	150.4
O3W−H1W3···Cl22	0.71(7)	2.66(7)	3.252(4)	142(6)	0.75	2.98	3.415(6)	120.4
O3W−H1W3···Cl23	0.71(7)	2.89(7)	3.361(3)	126(6)	0.75	2.81	3.317(6)	127.5
O3W−H2W3···Cl24#1	0.87(7)	2.30(7)	3.155(4)	170(5)	0.62	2.59	3.179(7)	161.9

Short Intermolecular Contacts

	100 K				293 K			
	D−H	H···A	D···A	D−H···A	D−H	H···A	D···A	D−H···A
N113−H113···Cl24#1					0.74	3.059	3.706	147.7
O1W−H2W1···Cl14					1.05	3.102	3.405	97.5
O1W−H2W1···Cl12#1					1.05	3.353	3.273	76.6
O2W−H1W2···Cl24#1	1.04	2.86	3.145	96.2				

[a] Symmetry transformations used to generate equivalent atoms: #1 $x, y, z - 1$; #2 $x, y, z + 1$.

take part in six and five hydrogen bonds. This may be a possible reason for differences in the higher values of the atomic displacement parameters in $(Cu2Cl_4)^{2-}$. Similar temperature behavior of the copper coordination tetrahedra, which are active centers in certain metalloproteins, was discussed by Bacci.[26] In such biomolecules conformational modification can influence the shape of the potential function of the active site.

Comparison of Hydrogen Bond Networks at Low and Room Temperatures. Considering the influence of temperature on the hydrogen bond network it can be noticed that the arrangement of two groups of atoms, N101, H101, Cl12, Cl13 and N201, H201, Cl14, Cl11, becomes slightly more symmetrical at room temperature in comparison to low temperature (Table 4). This is evidenced by increase of similarity in the distances H201···Cl14 and H201···Cl11 as well as the angles N201−H201···Cl14 and N201−H201···Cl11. The other change consists of the elongation of the N113···Cl24#1 contact from 3.575(3) Å at 100 K to 3.706(6) Å at 293 K which may be treated as vanishing of the bifurcation of the hydrogen bond with N113 as a donor atom. More significant modifications with the increase of temperature occur in surrounding of O1W water molecule which plays an important role as a link between different asymmetric units along *c*-axis. This molecule at low temperature is a proton donor in two bifurcated hydrogen bonds with Cl12#1, Cl11#1 (the last is rather a short contact than a bond) and Cl13, Cl14. It is also a proton acceptor in two bonds with O112 and O212. On passing to room temperature the contacts O1W···Cl14, O1W···Cl12#1 become more loose. At the same time it seems that the hydrogens of O1W reorganize into disordered positions, which are difficult to determine. Because of this behavior, the hydrogen atoms H1W1 and H2W1 were ascribed to presumable space-averaged positions which resulted in an unnatural O1W−H1W1···O212#1 angle (131.2°). In the case of O2W its hydrogen atom, H1W2, which at low temperature is involved in the hydrogen bond with Cl23 and in a short contact with Cl24#1, changes its position at room temperature with weakening of the bond with Cl23. The other hydrogen atom, H2W2, turns from its relatively weak interaction with Cl21#1 at low temperature to more linear one with Cl24#1. The hydrogen bonds of O3W with chlorine atoms are much less sensitive to the change of temperatures, except for some weakening of O3W−H1W3···Cl22 bond.

Structural Changes vs Temperature (PXRD Method). The X-ray powder diffraction patterns reveal two very interesting features. First is that the sample ground before the experiment has different lattice parameters than those obtained for the single-crystal sample. The observed pattern recorded at room temperature can be indexed with the same symmetry of the unit cell but with a doubled lattice parameter c. The second feature consists of dramatic dynamical changes in the intensities as well as in positions of some diffraction maxima with temperature. The greatest shifts are noticed for maxima with $l \neq 0$, those for $l > 2$ being the most significant. This behavior can be explained by changes in the hydrogen bonds which form a chain network along the *c*-axis. According to the discussed comparison of hydrogen bond network at low and room temperatures for the single-crystal structure one should emphasize that the system of these bonds shows certain plasticity and PXRD studies confirm that some rearrangements within the system (causing the mentioned doubling of the c parameter of the unit cell) take place even on gentle grinding. These changes may lead to a

(26) Bacci, M. *Chem. Phys.* **1984**, *88*, 39.

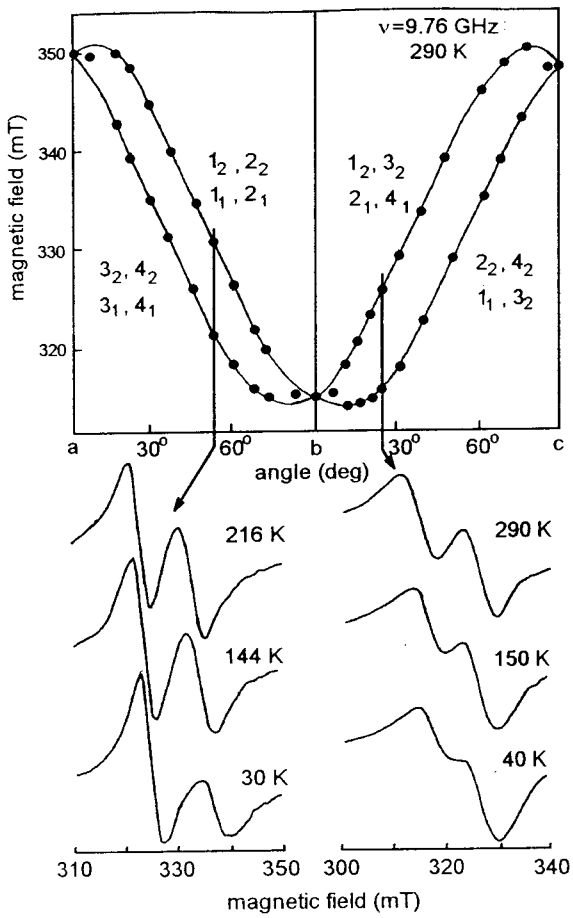

Figure 5. Angular variations of the EPR resonance field for two resolved lines in *ab* and *bc* crystal planes. The lines are composed of signals of the eight $(CuCl_4)^{2-}$ ions in the crystal unit cell marked as 1−4 with subscript 1 and 2 according to the Figure 2. Temperature evolution of the two line spectra for two selected crystal orientations is shown.

certain disorder along the same direction which seems to be very sensible to the mechanical and thermal effects.

Temperature Variations of EPR Spectra. In contrast with vast majority of Cu(II) compounds having a single EPR line, the EPR spectra of $[(cinH_2)^{2+}(CuCl_4)^{2-}]_2 \cdot 3H_2O$ show two splitted resonance lines at some crystal orientations. This means that the exchange coupling between inequivalent Cu(II) sites is very small although the hyperfine structure characteristic for magnetically diluted systems is not resolved but seems to determine the EPR line width as shown in the previous paper.[7] The line splitting appears in *ab* and *bc* lattice planes, where the expected eight lines from eight $(CuCl_4)^{2-}$ ions in the crystal unit cell should be reduced by crystal symmetry to two doublets from two geometrically different $(CuCl_4)^{2-}$-complexes marked in Figure 2 by subscript 1 and 2 of 1−4 molecules. However, only one doublet of approximately Lorentzian lines is observed in the both crystal planes as shown in Figure 5. This suggests that either 1_1 and 1_2, etc., type $(CuCl_4)^{2-}$-complexes have nearly identical orientations of their flattening deformation axes or the weak but EPR-detectable superexchange coupling operates in the crystal. We have performed computer simulations of the spectra using the algorithm including exchange-type coupling between paramagnetic centers producing two-line EPR spectrum.[27] The results show that the lines resolved in the *ab*-plane are not exchange coupled, thus each of the two lines is a superposition of four lines. However, the lines resolved in *bc*-plane are coupled by exchange interaction with exchange

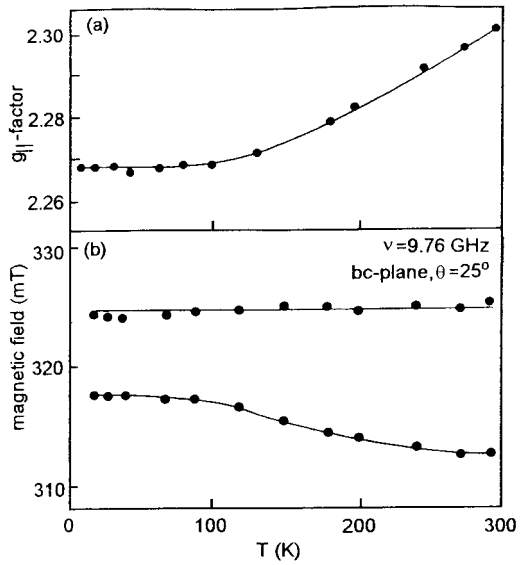

Figure 6. Temperature variations of the (a) $g_{||}$-factor and (b) resonance field of the lines split in *bc*-plane.

integral $J_{12} = 0.0030(5)$ cm^{-1}. This means that the lines in this plane represent exchange averaged spectra from geometrically inequivalent 1_1 and 1_2 sites. Because of the coupling the EPR lines of the crystal are formed by the whole asymmetric unit (pseudodimer) $[(cinH_2)^{2+}{}_2(CuCl_4)^{2-}]_2 \cdot 3H_2O$ with the anions differing slightly in the orientation. It is not often the case that a cluster consisting of two cations, two anions, and three water molecules and containing two magnetically inequivalent paramagnetic centers behaves as a separated magnetic unit in the crystal. It should be stressed that, besides the intramolecular J_{12} coupling, the weak superexchange operates also between magnetically equivalent sites and is transmitted by hydrogen bondings of water linked to these sites. This superexchange J_{11}, etc., which is not much weaker than J_{12}, works along *c*-axis and is responsible for smearing out of the hyperfine structure of the observed EPR lines.

Temperature variations of the EPR spectra (Figure 5) were recorded along two crystal orientations where the line splitting was maximum. Spectra vary smoothly with temperature due to a shift of the lines and the line broadening. Exchange coupling J_{12} is temperature independent while the *g*-factors vary with temperature. The $g_{||}$-factor variations evaluated from the powder EPR spectrum are shown in Figure 6a, and the shift of the lines in the *bc*-plane of the single crystal is shown in Figure 6b. Continuous shift of the *g*-factors from $g_{||} = 2.292$ and $g_{\perp} = 2.051$ at room temperature to 2.268 and 2.047 at 10 K, respectively, shows that the flattening angle β of the $CuCl_4$-tetrahedra increases on cooling as predicted by the crystal field theory of distorted tetrahedral Cu(II) complexes.[28] The increase in β-angle in the whole temperature range can be evaluated from *g*-factor shift as of about 3° using theoretical data of the previous paper.[7] The increase is comparable with the Deformation parameter shown in Table 2. This compression of the tetrahedra is due to an increase in the strength of the hydrogen bonds in which chlorine atoms are involved as discussed in the previous section. The hydrogen bonding withdraws the electron density from the chlorine ions, allowing the crystal field to dominate over the Cl−Cl electrostatic repulsion. It leads toward the more

(27) (a) Hoffmann, S. K.; Hilczer, W. *Inorg. Chem.* **1991**, *30*, 2210. (b) Hoffmann, S. K.; Hilczer, W.; Goslar, J. *Appl. Magn. Reson.* **1994**, *7*, 289.

(28) Hoffmann, S. K.; Goslar, J. *J. Solid State Chem* **1982**, *44*, 343.

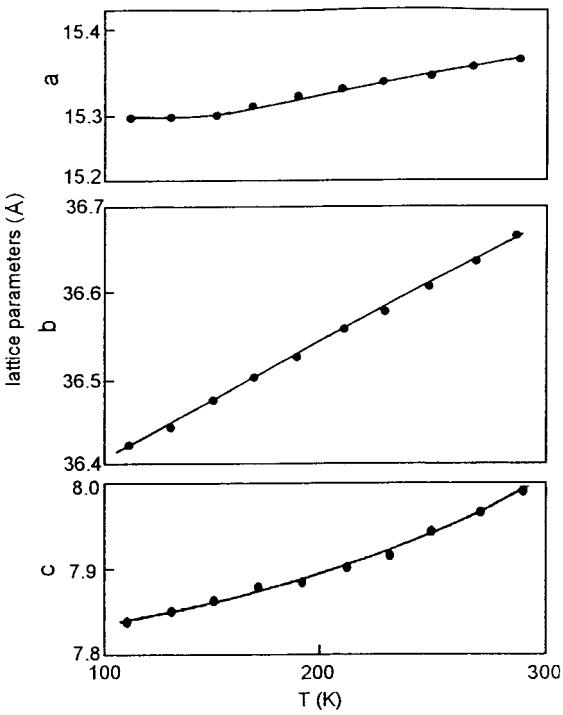

Figure 7. Temperature variations of the crystal unit cell parameters. Thermal expansion coefficients are practically constant along *a* and *b* axis with $(\partial a/\partial T) = 2.3 \times 10^{-5}$ Å K^{-1}, $(\partial b/\partial T) = 3.7 \times 10^{-5}$ Å K^{-1}, whereas the coefficients along *c*-axis grow linearly with temperature from 4.5×10^{-5} Å K^{-1} at 130 K to 7.7×10^{-5} Å K^{-1} at 290 K.

planar geometry. This effect is also seen as the change of the color of the sample from yellow green to green at low temperatures due to a small blue shift of the absorption d−d band.

Thus, although the X-ray data collected at two temperatures could suggest that the increase of temperature causes a reorganization of the hydrogen bond network, the EPR data clearly show that continuous changes of $(CuCl_4)^{2-}$ geometry appear in the whole temperature range. The continuous character of the temperature $(CuCl_4)^{2-}$ deformations is confirmed by thermal expansion data (Figure 7). Monotonic increase in the crystal unit cell parameters *a*, *b*, and *c* with temperature does not show any structural phase transition in the whole temperature range. Moreover, the largest linear thermal expansion coefficient appears along *b*-axis, i.e., in the direction perpendicular to the 1−2 and 3−4 layers (see "cages" in Figure 2) as should be expected. The thermal compression along the *a*-axis stops at low temperatures when the new water mediated hydrogen bond is formed which leads to a more rigid structure along the *a*-axis.

Conclusions

The $[(cinH_2)^{2+}(CuCl_4)^{2-}]_2 \cdot 3H_2O$ crystal shows weakly thermotropic behavior in the whole temperature range due to a flexibility of $(CuCl_4)^{2-}$ structure which can be modified by temperature variations of the strength of the bifurcated hydrogen bonds.

The conformation of the cinchonine cation in the vicinity of the O12, C8, C9, and C16 atoms is relatively stable with temperature except for the H12−O12−C9−C8 torsion angle which is very sensitive to the increase of temperature. The quinuclidine moiety behaves analogously, except for the very labile vinyl moiety. Cations and anions in the asymmetric unit are interconnected by the hydrogen bonds arranged approximately in the ab plane. The $(CuCl_4)^{2-}$ tetrahedra are linked with the water molecules, along *c*-axis, mainly via hydrogen bonds. This subtle network of hydrogen bonds changes with temperature most probably due to the slight rearrangement of the water molecules. This effect was also observed for pollycrystalline samples both on grinding and cooling.

Very weak exchange interaction operates in the crystal. The interaction couples geometrically inequivalent $(CuCl_4)^{2-}$-tetrahedra in $[(cinH_2)^{2+}(CuCl_4)^{2-}]_2 \cdot 3H_2O$ and as a result the whole asymmetric units corresponding to the general chemical formula of the compound behave as an individual magnetic units (pseudodimers). These units are also coupled into a layer parallel to the *ac*-plane by a weak superexchange smearing hyperfine structure of the EPR spectra.

Acknowledgment. A.W.-B. is thankful for financial support from Jagiellonian University (CRBW). The authors are grateful to Dr. hab. K. Stadnicka for guiding assistance in the diffractometric measurements.

Supporting Information Available: Full listings of crystal data, details of data collection and structure refinement, atomic coordinates, bond lengths and angles, torsion angles, anisotropic displacement parameters, hydrogen coordinates and isotropic displacement parameters, and hydrogen bond parameters (CIF files). This material is available free of charge via the Internet at http://pubs.acs.org.

IC001402A